Spectrochimica Acta Part A: Molecular and Biomolecular Spectroscopy 259 (2021) 119881

Contents lists available at ScienceDirect

Spectrochimica Acta Part A: Molecular and Biomolecular Spectroscopy

journal homepage: www.elsevier.com/locate/saa

Bisphenol–based cyanide sensing: Selectivity, reversibility, facile synthesis, bilateral "OFF-ON" fluorescence, C_{2v} structural and conformational analysis

Zakir Ullah [a,b], Prasad M. Sonawane [a], Thien S. Nguyen [c], Mousumi Garai [b], David G. Churchill [a,d,*], Cafer T. Yavuz [a,b,c,*]

[a] Department of Chemistry, Korea Advanced Institute of Science and Technology (KAIST), Daejeon 34141, Republic of Korea
[b] Graduate School of Energy, Environment, Water and Sustainability (EEWS), KAIST, 291 Daehak–ro, Yuseong–gu, Daejeon 34141, Republic of Korea
[c] Advanced Membranes and Porous Materials (AMPM) Center, Physical Science & Engineering, King Abdullah University of Science and Technology (KAUST), 4700 Thuwal, 23955–6900 Kingdom of Saudi Arabia
[d] KAIST Institute for Health Science and Technology (KIHST) (Therapeutic Bioengineering Section), 291 Daehak–ro, Yuseong–gu, Daejeon 34141, Republic of Korea

GRAPHICAL ABSTRACT

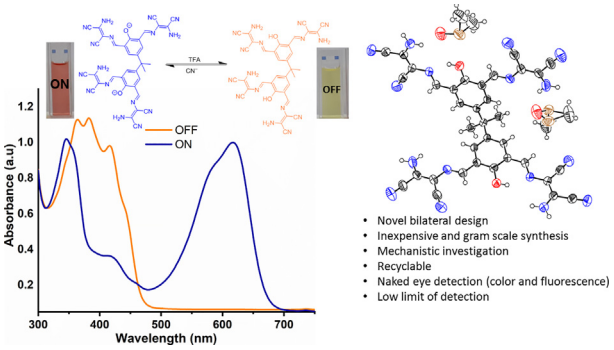

ARTICLE INFO

Article history:
Received 7 March 2021
Received in revised form 18 April 2021
Accepted 22 April 2021
Available online 26 April 2021

Keywords:
Cyanide ion detection
Bisphenol
Chemosensing
Reversible
On-site economical application
^{1}H NMR
UV–Vis spectroscopy

ABSTRACT

A structurally characterized novel dual–pocketed tetra–conjugated bisphenol–based chromophore (fluorescence = 652 nm) was synthesized in gram scale in ~90% yield from its tetraaldehyde. Highly selective, naked-eye detection of CN^- ($DMSO/H_2O$) was confirmed by interferent testing. A detection limit of 0.38 μM, within the permissible limit of CN^- concentration in drinking water was achieved as mandated by WHO. The "reversibility" study shows potential applicability and reusability of **Sen**. Moreover, cost-effective and on-site interfaces, application tools such as fabricated cotton swabs, plastic Petri dishes, and filter papers further demonstrated the specific selectivity of **Sen** for the toxic CN^-. In addition, an easily available and handy smartphone-assisted "Color Picker" app was utilized to help estimate the concentration of CN^- ion present. A dual phenol deprotonation mechanism is active and supported by ^{1}H NMR spectroscopic data and DFT calculation results.

* Corresponding authors.
E-mail addresses: dchurchill@kaist.ac.kr (D.G. Churchill), cafer.yavuz@kaust.edu.sa (C.T. Yavuz).

https://doi.org/10.1016/j.saa.2021.119881
1386-1425/

1. Introduction

Ions have a great impact on our life, as numerous biological and industrial processes depend on the presence and transport of ions, and in particular, *anions* [1,2]. The development of small molecule anion sensors and probes has been an area of significant attention over the past 30 years [3–5]. Fluorescence and calorimetry continues to receive attention. As there is no perfect single probe for any one analyte, this area of research has been driven by the important roles anions play in industrial processes and biology, and the prospective lucrative market for the selective sensing of analytes for either biological purposes or those relating to the environment. The need, therefore, to explore new chemical and physical methods of sensing anionic pollutants in the environment helps drive research endeavours, and the synthesis and study of new chromophores as well as the exploration of receptor combinations which often take the shape of supramolecular and multimeric designs, and in some cases, polymeric designs. This leads to new scientific assay trials and allows eventually for new applications of such probes. Chromophores can be conjugated with active sites that can interact with a wide variety of analytes and simulants [6].

The behavior of even small molecule probes may be especially complex sometimes in that they might aggregate or bind to other targets in biology, or respond unexpectedly to pH changes [6,7]. In particular, the synthesis of the optimization of colorimetric anion sensors is of great importance; visual detection can offer both important qualitative and quantitative information. The chemical design of receptor sites for anions has seen a lot of research activity [8]. The cyanide ion (CN^-) is a conjugate base of weak acids (pK_a of HCN = ~9.2). The probes designed to detect these ions may also be sensitive to H^+ and OH^- concentration (*vide infra*).

The cyanide ion is an ion of concern: prevalent and with roles that are natural and roles that present environmental contamination concerns. CN^- imparts adverse effects which are notoriously severe upon human or other exposure. The biology of CN^-, as featured in certain bioinorganic chemistry systems can cause serious pollution in water; foods such as bitter almonds, potatoes, and cassava are regarded as poisonous because of the levels of analyte(s) present. Additionally, if the CN^- ion, in the form of cyanogenic glycosides, exceeds 200 ppm, then toxicity becomes a problem for human health [9]. The Environmental Protection Agency (EPA) and the World Health Organization (WHO) have defined the maximum CN^- limit in drinking water as 0.2 ppm and 1.9 μM, respectively [10–12].

Substantial strength has been made to design donors/receptors containing functionalities that comprise imine [13–15], phenol [16–18], amide [19–21], urea [22–25], thiourea [26,27], imidazole [28] pyrrole [29,30] and 1,3,4–oxadiazole subunits [31,32]. The chromophore–conjugated receptors favorable to anions have features that are usually in contrast to those for metal ions and cations. Hydrogen–bonding often features strongly in these aforementioned receptor pockets and will relate to the chemical mechanism at play [33]. The photophysical signaling mechanisms include excited-state proton transfer (ESIPT), internal charge transfer (ICT) [34,35], and photoinduced electron transfer (PET) [36].

When considering such intended probing, rich solvent differences exist which effect the sensing potential of fluorophores and receptors. The DAMN functionality is a reliable moiety. There have been a number of synthetic reports for the DAMN functionality used in heterocyclic synthesis [37]. These synthetic approaches have impacted our present scientific approach and analysis. Herein, a simple, sensitive, and selective cyanide anion colorimetric sensor-based detection is presented and discussed in which the sensor is a soluble tetra-Schiff base system in which DAMN groups have helped form a tetra-conjugated species.

2. Materials and methods

All solvents and chemicals were either of analytical grade or spectroscopic grade. Tetrabutylammonium salts were purchased from Sigma Aldrich and used without further purification. NMR spectra were recorded on a Varian 400 MR spectroscope in DMSO–*d6* and $CDCl_3$ as the NMR solvent. Absorption spectra were measured by using a Shimadzu 1280 ultraviolet–visible spectrometer at room temperature. A PerkinElmer LS 55 instrument was used for fluorescence studies. The fluorescence spectra were recorded with an excitation wavelength of 652 nm and a 5 nm slit.

2.1. Synthesis of 5,5′–(propane–2,2–diyl)-bis-(2–hydroxyisophthaldehyde)

Hexamethyltetraamine (HMTA) (14.01 g) was added to trifluoroacetic acid (TFA); then, bisphenol (4.5 g) was added to the reaction mixture. The reaction mixture was then heated to 120 °C and maintained at that state for 16 h. After that time, the reaction mixture was then cooled to 100 °C whereupon 50 mL of 6 M HCl was then added. The reaction mixture was then stirred for 3 h at 100 °C. After this time, the reaction mixture was cooled to room temperature and a small portion of water was added helping create a precipitate. The precipitate was then extracted by using dichloromethane and water; the organic layer was deliberately concentrated by way of rotary evaporation to afford isolation of the desired *tetraaldehyde* intermediate (**1**) compound (5,5′–(propane–2,2–diyl)bis(2-hydroxyisophthaldehyde) for further reaction without purification.

2.2. Synthesis of Schiff base ***Sen***

The tetraaldehyde produced above **(1)** was then directly used for the synthesis of the Schiff base product **(Sen)**. The tetraaldehyde 5, 5′–(propane–2, 2–diyl)bis(2-hydroxyisophthalaldehyde) (1.00 mmol, 340 mg) was dissolved in 10 mL of CH_2Cl_2 solvent. Next, the diaminomaleonitrile reagent (DAMN) (4.00 equiv, 432 mg) was added to the reaction mixture. Furthermore, three to four drops of concentrated sulfuric acid were then added as a catalyst; the reaction mixture was stirred for 24 h at room temperature. An orange precipitate formed and was filtered out, and then washed with methanol (MeOH) to help remove all impurities present. ^{1}H NMR (300 MHz, DMSO d_6): 1.79 (s, 6H, Methyl), 7.96 (s, 4H, Aromatic), 8.04 (s, 8H, NH_2), 8.61 (s, 4H, —HC═), 11.42 (s, 2H, —OH). ^{13}C NMRS (100 MHz, DMSO d_6) δ: 30.66 (C_1), 42.15 (C_2), 103.25 (C_3), 114.92 (C_4), 121.36 (C_5), 126.97 (C_6), 132.25 (C_7), 142.15 (C_8), 154.72 (C_9), 157.01 (C_{10}). HRMS (ESI): calcd for $C_{35}H_{24}N_{16}O_2$: 700.2268; found: *m*/*z* 701.2415 (M + H) $^+$.

2.3. Theoretical methodology

All electronic structure calculations were carried out using density functional theory (DFT) with a hybrid functional B3LYP together with the DFT-D3 method for considering dispersion interactions [38] and well-accepted basis sets: 6-311+G** and 6-31++G** as implemented in Gaussian 16 [39]. All calculations were performed at default temperature and pressure settings (298.15 K and 1.00 atm). The conductor-like polarizable continuum model (CPCM) method was used to apply the solvent effects in the calculations. Furthermore, the frequency calculations have been carried out to confirm the nature of the obtained minima at the same level of theory as that for the geometry optimizations. The UV–Vis spectra simulations were performed at the time-dependent (TD), TD-CAM-B3LYP/6-311++G** level of theory [40].

3. Results and discussion

In our present approach, starting with bisphenol A (**1**), we built out a bilateral design involved in keeping two sides of the probe identical and available, allowing for a dual detection, to help effect a form of bilateral detection (Scheme 1) (*vide infra*). The bisphenol core imparts a C_{2v} molecular symmetry. The chemistry involves the formation of four imine groups in total, and leaves from equivalent amine groups unreacted. An organic synthesis approach using the condensation reaction is provided for the target compound (**Sen**). The basic experimental approach for the synthesis of the DAMN–based optical sensor is illustrated in Scheme 1. First, bisphenol A was acquired commercially and was treated with hexamethylenetetramine (HMTA) in the presence of trifluoroacetic acid (TFA) at 120 °C for 16 h. The corresponding tetraaldehyde (**2**) was collected as a precipitate upon cooling the reaction mixture to room temperature. The aldehyde was confirmed to be produced (85% yield) and was then treated with diaminomaleonitrile (DAMN) at room temperature, in dichloromethane solvent and sulphuric acid (the catalyst) to help afford the corresponding multiple Schiff base–containing product. This optical sensor was then purified with methanol and collected as a yellowish solid in 90% overall yield. The reaction at one DAMN amine appear to deactivate the remaining DAMN amine, which would otherwise lead to the production of polymeric (dendritic) molecular forms.

Impurities present (estimated to be un–reacted DAMN) are washed away with methanol. There is no current evidence of polymer formation at present, as viewed by mass spectrometry and single crystal structural analysis (Figs. S5 and S6). The proportions in the chemical groups of the synthesized optical sensor **Sen** were confirmed by analysis afforded by inspecting the ^{1}H and ^{13}C NMR spectra (Figs. S1 and S2). The FT–IR spectra of the sensor bisphenol and DAMN groups are also compared (Fig. S3). Finally, the single-crystal diffraction successfully determined the product **Sen** allowing for a detailed comparison between it and related structures (CCDC 2053281). The X-ray diffraction study was highly useful in confirming both that (i) the desired product was cleanly generated and also (ii) in helping understand preferred DAMN conformations and therefore in better understanding the preferred hydrogen bonding tendencies of both pockets. The intermolecular packing (Fig. S8) and solvent molecules (DMSO) present provide a more complete picture of the aggregation possibilities of molecules such as **Sen**.

3.1. The spectroscopic properties of compound *Sen* and its optical response to CN^-

The maximum absorbance and emission of Sen in 50% DMSO/H_2O were assigned at 407 and 652 nm, respectively, in the presence of the CN^- ion. The selectivity study of Sen to detect different anions was carried out (F^-, Cl^-, Br^-, CN^-, I^-, AcO^-, $H_2PO_4^-$, BF_4^-, ClO_4^-, HSO_4^-, NO_3^-, S^{2-}); (Fig. 1b) at an excitation wavelength of 520 nm. From the contents of Fig. 1a and 1b, it can be seen that Sen is selectively detecting CN- ion over other relevant competitive anions with the noteworthy color change being from pale yellow to red. Hence it can be used as a powerful tool to detect CN- ion by a naked eye considering the solvent system chosen.

We measured the maximum absorption of **Sen** (30 μM) before and after the CN^- ion added in 50% aq. DMSO media (Fig. 2a). In the beginning, without the addition of the CN^- ion, **Sen** exhibited an absorption band at 407 nm as depicted. As soon as the CN^- ion addition started, there is a continuous decrease in the absorbance at peak 407 nm and a concomitant increase in the absorption band at 520 nm, whereas the color of a sample changes remarkably from pale-yellow to red. In addition, an isosbestic point was observed at appx. 445 nm.

Besides, to evaluate the potent ability of **Sen** to help quantify CN^- ion, a titration study was performed with the incremental

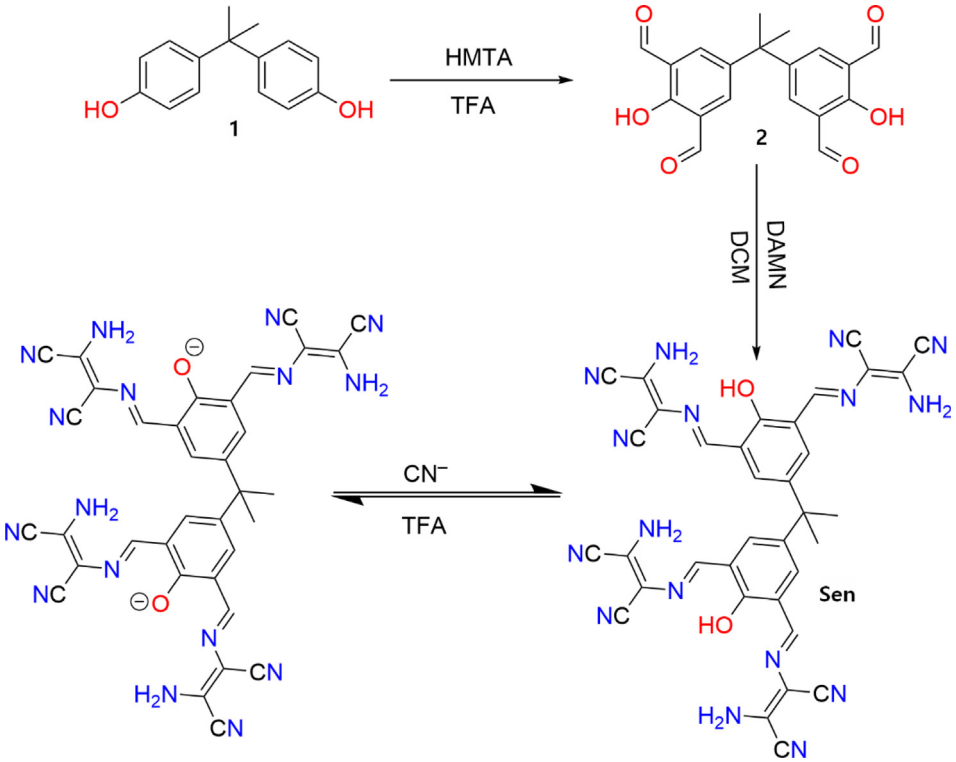

Scheme 1. Synthesis of **Sen** and its chemical switching with selective analytes.

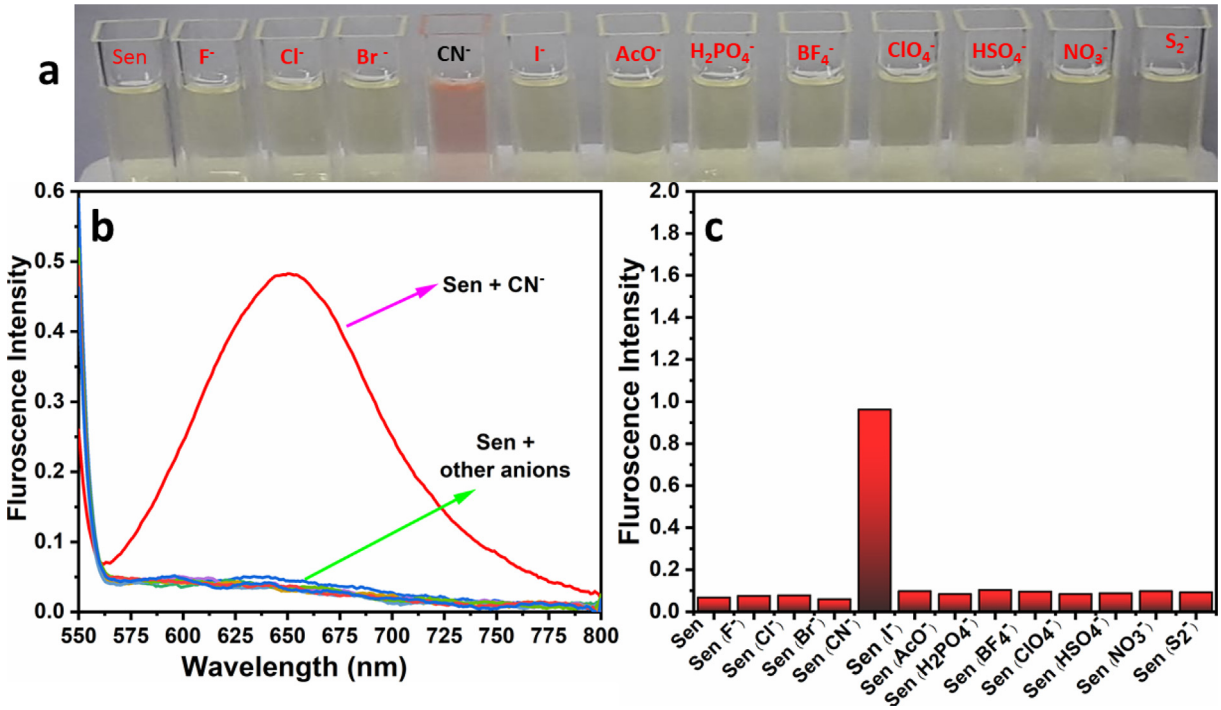

Fig. 1. (a) Naked eye detection, (b) emission spectra of **Sen** (30 μM) with CN^- (2 equivalent) and the other anions (10 equivalent), (c) relative emission spectral analysis.

addition of the CN^- ion with **Sen** (30 μM) in 50% aq. DMSO solution (Fig. 2a). Before the addition of the CN^- ion, **Sen** (30 μM) centered a broad emission wavelength at 652 nm when excited at a wavelength of 520 nm. The peak at 652 nm progressively increases upon incremental addition of CN^- ion (0–60 μM) with a red-shift observed and it induced a 22-fold enhancement in the original emission intensity. The maximum intensity has been obtained upon the addition of 2 equivalents of CN^- ion. A good linear relationship was observed after the addition of CN^- ion in the range of 0–60 μM (Fig. 2c). Further addition of more equivalents of CN^- ion not show any observable further enhancement in the emission intensity. This experiential "turn-on" response endorses the prevention of the ICT mechanism thought to be present with **Sen**. The recognition limit was identified as 0.38 μM, r = 0.99, (Fig. 2c), this value is much lower than the tolerable level of CN^- ion in drinking water as mandated by the WHO (1.9 μM). Job plot analysis was recorded and measured to be 0.33 indicating a 1:2 stoichiometry relationship between **Sen** and the CN^- ion (Fig. 2d). Moreover, from the renowned Benesi-Hildebrand equation, the association constant (Ks) was computed to be $1.08 \times 10^9\ M^{-2}$ (Fig S13).

3.2. Interference study

Further, to examine the interference of other anions, the interference study was recorded after addition of various anions (F^-, Cl^-, Br^-, CN^-, I^-, AcO^-, $H_2PO_4^-$, BF_4^-, ClO_4^-, HSO_4^-, NO_3^-, S_2^-) with **Sen** (30 μM) in 50% aq. DMSO solution and in the presence of 2 equivalents of CN^- ion. From Fig. S9, it has been clearly seen that even though (300 μM) of other competitive anions is added, this does not force the change in fluorescence emission intensity of **Sen** in presence of the CN^- ion. This outcome made evident that no other competitive anions exhibits any interference in order to help sense CN^- ion.

A deeper appreciation of the deprotonation that appears to trigger the optical change, and therefore the sensing event, was pursued by a variable pH study both experimentally and theoretically. We were able to address this issue conveniently by DFT/TD–DFT calculation methods which affirmed UV bands (Fig. 3a and 3b) existed and were comparable, albeit approximately to those obtained experimentally [41]. The removal of one phenol proton, followed by another in sequence, results in, at first, a red shift and then a doubling of the absorption at the value of 522 nm. Therefore, we consider one phenol subunit bearing two DAMN units to be operating independently from the other phenol subunit present in **Sen**. Through the DFT study especially upon deprotonation, the band reveals both an increase in π–delocalization which contributes to red shifting; the second deprotonation helps increase the intensity of the new band at 522 nm as if it were coming from a second unattached molecule (*vide infra*).

To ascertain the uniqueness of our system better, we sought to establish the detection limit for cyanide ions tested by using various concentrations of salt solutions of the corresponding anion (Fig. 2c). The limit of detection was analysed by varying the concentration of the corresponding anion salts from 0 to 60 μM. This helped establish an understanding of how the probe behaves amidst a dynamic range. One difference between our probe and others reported in the literature is that, from the outset, there are two identical binding pockets. Because of the way the chemical groups are geometrically directed, with small analytes, the DAMN arm of one phenol group cannot be expected to join forces with a DAMN arm of a different phenol arm regarding a small molecule analyte such as CN^-; both sides, to the best of our knowledge can, in turn, be fully involved in the detection of the same analyte in which there is total loading of 2 equiv.

We first looked at the sensing mechanism enabled by the monomeric version of **Sen** which was synthesized and previously reported [42]. We referred to this report and prepared an authentic sample for this; the NMR spectrum and IR spectra are both closely akin to those for **Sen** (Figs. S1, S4, and S7). This suggests that **Sen** loads one side, then the other, in turn. However, interestingly, in the bisphenol–based probe binding, one pocket/side might strongly change the physical properties of the entire molecule so

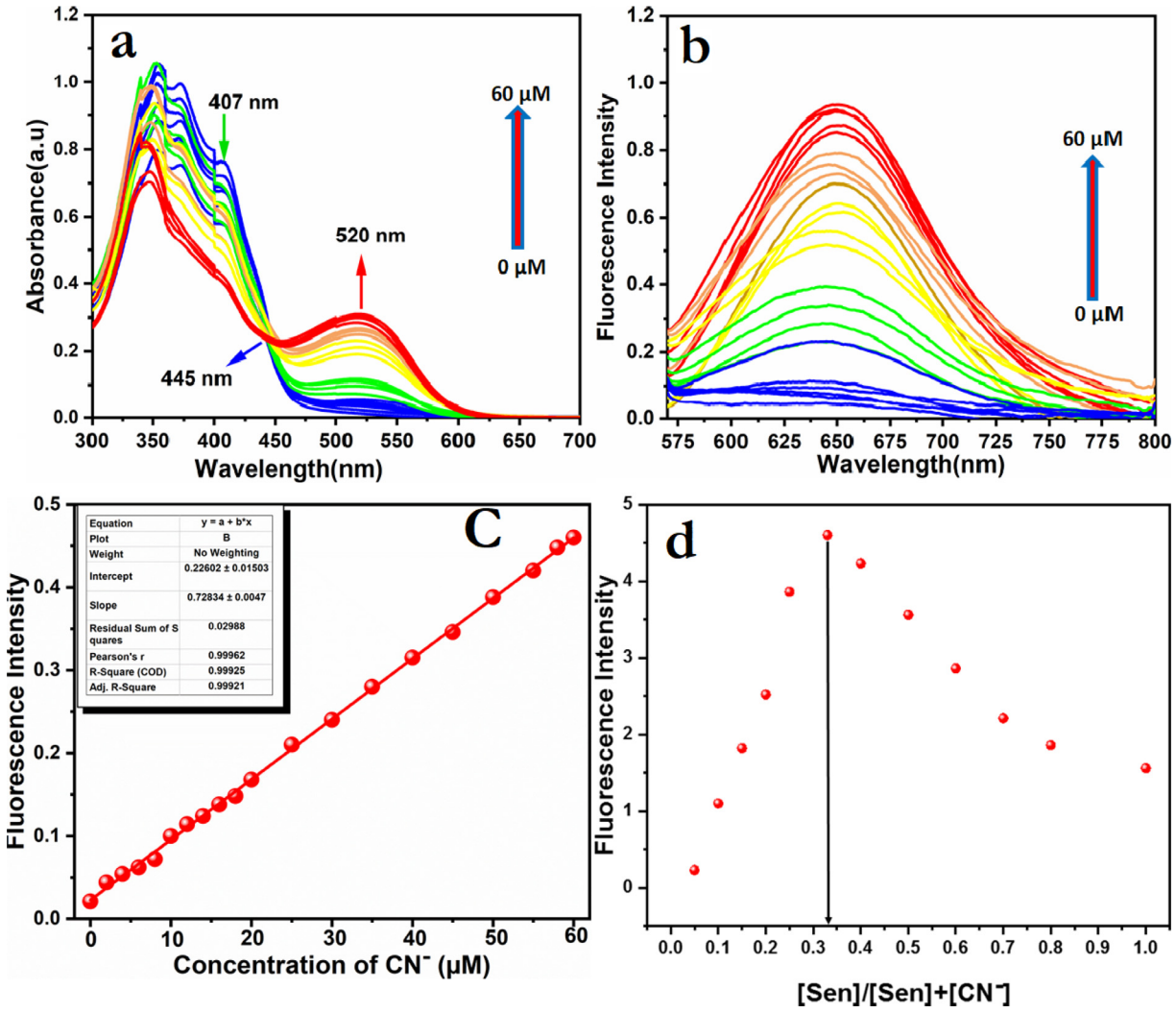

Fig. 2. (a) UV–Vis spectra change in **Sen** (30 µM) upon addition of CN^- ion (0–60 µM), (b) emission spectra of **Sen** (30 µM) with the CN^- ion (0–60 µM), (c) calibration curve for the calculation of the detection limit of **Sen** (30 µM) upon addition of CN^- ion (0–60 µM), (d) Job plot revealing the expected 1:2 stoichiometry relationship of **Sen** with CN^- ion.

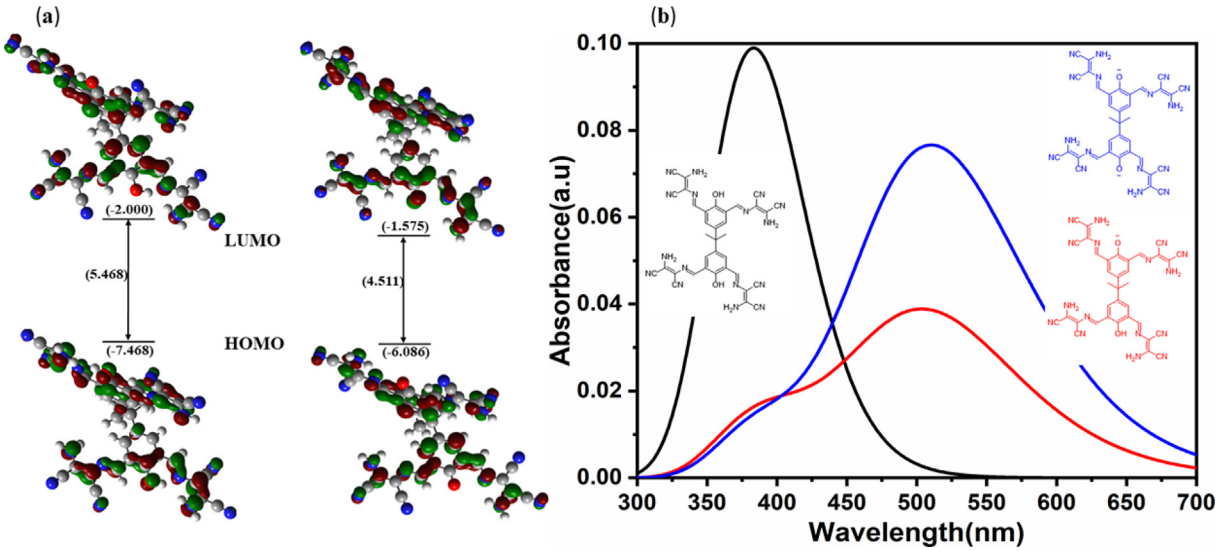

Fig. 3. (a) Frontier molecular orbital analysis of **Sen** and **Sen**$^{-2}$, (b) calculated UV–Vis spectra of **Sen**$^{-1}$ and **Sen**$^{-2}$.

that (**Sen** [CN^-]) bears different solvation properties and/or charge properties, etc. This is represented by the results of our DFT/TD–DFT $SenH^-$ structure (Fig. 3b). Furthermore, in contrast to **Sen**, the isosbestic point was observed at 445 nm, suggestive of no reaction intermediate being present. The corresponding **Sen** intersection point is not crisp, suggestive of the fact that it is singly loaded and this singly loaded species is therefore an intermediate before doubly loading is effected. Interestingly, we suggest that the two sides operate fully independently, but the preferred environment of the second analyte uptake and probe polarity may be swayed by the presence of the first analyte and formation of **Sen** [CN^-]. This bilateral probing may be an issue for further research.

Regarding the photomechanism, the emission spectra were observed only for the **Sen** which was charged with the CN^- ion only. The DFT/TD–DFT calculations also helped us to examine the emission characteristics to attempt to determine the photomechanism at play, which presently is strongly supported as being internal charge transfer (ICT). This photomechanism which operates from an electron *donor* to an electron *acceptor*, conjugated without spacer. The dipole moment therefore became enlarged. ICT causes significant shifts in the absorption and emission bands, which reflects the strength of the **Sen**–CN^- interaction.

3.3. pH study

In order to investigate the effect of pH on **Sen** with and without the CN^- ion added, the fluorescence intensity was measured at different pH values (Fig. 4b). The fluorescence intensity was recorded with or without the addition of two equivalents of CN^- ion. The outcomes obtained from this experiment showed that the fluorescence intensity of Sen after the addition of CN^- ion was markedly enhanced in a wide range of pH values (5–10) without the interference of the hydroxide. This shows the potential efficiency of **Sen** in order to help detect CN^- ion in the wide range of pH (5–10). This allows **Sen** to be suitable for biological applications. The incremental changes observed in the fluorescence intensity of **Sen** without the addition of CN^- ion after pH 5–10, indicates that the hydroxide ion may be helping deprotonate the phenol proton (—OH). Next, the fluorescence intensity of **Sen** observed at a pH of more than 10 and 11 of **Sen** (50% aq. DMSO media) with and without CN^- ion added, shows nearly the same values indicating that the mechanism of **Sen** in order to detect the CN^- ion may consist of the deprotonation of phenol proton (—OH). This suggests that in the strong basic media such as pH > 10, further addition of CN^- ion has no further effect in the enhancement of probe fluorescence intensity due to saturative deprotonation of both phenol (–OH)

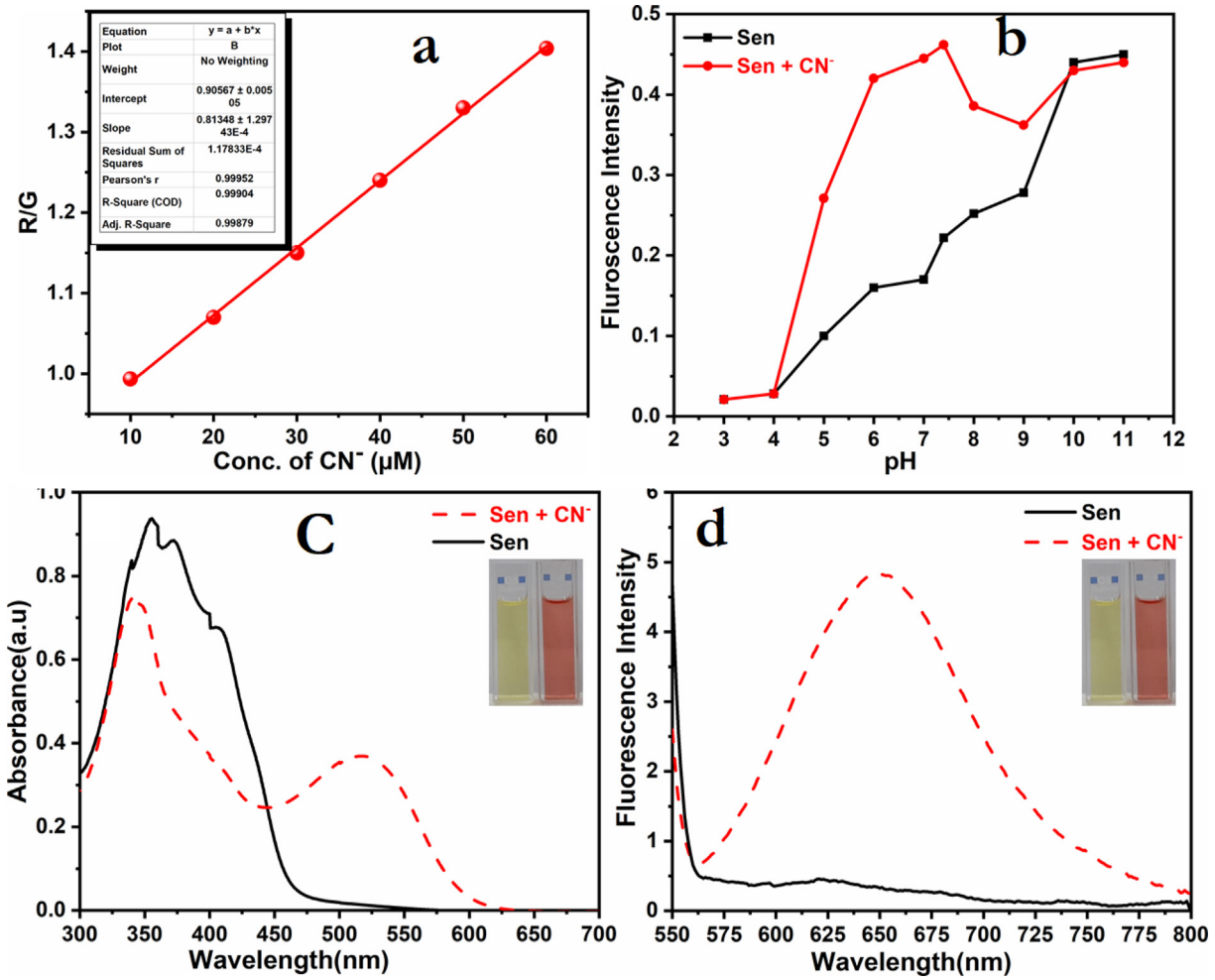

Fig. 4. (a) Smartphone–assisted RGB response for the determination of CN^- ion, (b) The effect of the pH on **Sen** (30 μM) with the CN^- ion (60 μM), (c) UV–Vis absorption spectrum of **Sen** (30 μM) upon addition of the CN^- ion (60 μM), and (d) emission spectra of **Sen** (30 μM) with the CN^- ion (60 μM).

groups by the hydroxide ion. Moreover, a freely available "Colour picker App" was utilized; changes in the value of RGB were calculated upon incremental addition of CN^- ion. Finally, as shown in Fig. 4a, the ratio of R/G Vs. the concentration of the CN^- ion was plotted. The good linearity range (r 0.99) and LOD (0.34 μM) were obtained. The LOD was determined to be 0.38 μM, measured by fluorometric titration studies (Supporting Information). This approach represents the possibility of on-site detection of CN^- ion with a low cost and convenient smartphone app.

3.4. On-site practical application

We examined the practical employability of **Sen** to help detect CN^- ion with a simple affordable plastic petri dish, Whatman filter paper tests, and cotton swabs. Noteworthy, it was found that all media above were simple and on-site techniques that were highly useful to help detect CN^- ion by simple and observable color changes from pale yellow to red. In the case of cotton swabs, at first, commercially and easily available cotton swabs were immersed in a stock solution of **Sen** in DMSO before being dried well in the air prior to its applicability. Subsequently, these air-dried and well-coated **Sen** cotton swabs were dipped into aqueous solutions of various anions (F^-, Cl^-, Br^-, CN^-, I^-, AcO^-, $H_2PO_4^-$, HSO_4^-, NO_3^-, S^{2-}).

Remarkably, it was observed that only the cotton swab soaked in an aqueous solution of CN^- ion showed a visible red color (Fig. 5a). On the other hand, other competitive anions showed a pale yellow result. This experiment, with distinguishing color changes from pale yellow to red, points out that the simple practical utility of **Sen** to help detect the toxic CN^- ion which can become a very useful colorimetric tool in the tool kit for on-site detection of CN^- ion. Commercially available plastic Petri dishes were utilized for this purpose to see the observable color changes from pale yellow to red with one's naked eye upon incremental addition (presence) of CN^- ion. Initially, **Sen** (30 μM) in 50% aq. DMSO solution was poured into the plastic Petri dish followed by the incremental addition of CN^- ion (10, 20, 30, 40, 50, 60 μM). From Fig. 5b, it is observed that the color of the solution detection was changed from pale yellow to red making evident its ability to help sense toxic CN^- ion in different situations. Succeeding, for more simple employability of **Sen**, we dipped the commercially available Whatman filter papers into various concentrations of CN^- ion solutions (10, 20, 30, 40, 50, 60 μM) with Sen (30 μM) in 50% aq. DMSO and then dried well. A similar observation was found, in the case of the plastic Petri dishes. They give a distinguishable color change from pale yellow to red by the naked eye as depicted in Fig. 5c. Therefore, all the above simple, affordable and practical colorimetric tools indicate the potential applicability of **Sen** to help detect toxic CN^- ion.

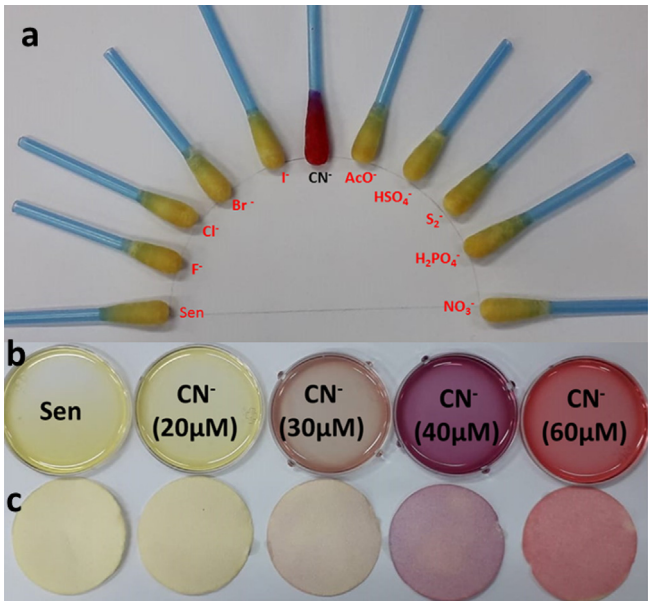

Fig. 5. (a) A simple on-site technique involving cotton swabs being used for naked eye visualization of CN^- ion with **Sen** and other anions. (b and c) (top) Petri dish and (bottom) Whatman filter paper techniques for the naked eye color change visualization of incremental concentration of the CN^- ion (0–60 μM) with **Sen** (30 μM).

3.5. Proposed sensing mechanism

The sensing mechanism was tracked with ^1H NMR spectroscopy: The **Sen** (10. mg, 0.010 mmol) was dissolved in 1.0 mL DMSO–d_6. The anion salt TBACN (0.028 mmol) was then added, respectively. With the addition of TBACN, the OH spectral peak was not present in the ^1H NMR spectrum; this supported deprotonation had been affected. Upon the addition of 0.5 μL of trifluoroacetic acid (TFA), the color of the corresponding **Sen** + CN^- changed back to yellow (from blue) and the spectral peak of OH was observed this shows that the re–protonation of the **Sen** was made. Again, by adding TBACN to the same mixture, the color changed back to blue, and the OH proton disappeared in the ^1H NMR spectra.

3.6. Reversibility study

Next, the issues of analyte detection reversibility and reusability with **Sen** were addressed, based on the emission spectrum observations (Fig. 6a and 6b). To help determine both the reversibility and reusability of **Sen**, we carried out titration and reversibility switching cycle experiments.

In order to investigate the chemical reversibility property of **Sen**, we performed reversibility studies by alternative addition of CN^- ion and TFA for 5 cycles as depicted by Fig. 6a and 6b. All "reversible" titrations were performed in 50% aq. DMSO solution; their respective fluorescence emission intensity was recorded. In the beginning, 2 equivalent of CN^- ion was added to **Sen** (30 μM) in 50% aq. DMSO solution which exhibited a pale yellow color which are immediately turned to red. Remarkably, it was noted that the relative emission intensity upon the addition of CN^- ion was increased at a wavelength centered at 652 nm. This may be due to the deprotonation of phenol (—OH) by the CN^- ion. On the other hand, noteworthy reversible and visible colorimetric changes were observed from red to pale yellow after the addition of H^+ ion source, TFA (30 equiv.). The reason may be due to negatively charged **Sen** protonated after addition of H^+ ion source such as TFA which turns into a decrease in florescence emission intensity at 652 nm. This alternative addition of CN^- ion followed by H^+ ion source such as TFA was performed 5 times; a small decrease in the fluorescence emission intensity in the reversible cycle of CN^- ion and H^+ ion source TFA was observed. This reversibility study evidenced the promising feature of recycling and reusability of **Sen** in order to help detect toxic CN^- ion.

Lastly, based on the success with acquiring a structural study, conformations of **Sen** were explored. **Sen** exhibits different bond rotations that allow for different conformations as well as possible isomers. The conjugated DAMN arms dangle from each side and invite a conformational analysis in which the ensemble of both single and double bonds are rotated in turn by 180°. While, there are a great possible number of different structures to analyse, we studied some of these isomers determined by DFT conformational approaches (Fig. 7), which involved both single pointing, and frequency calculations (see Fig. 8).

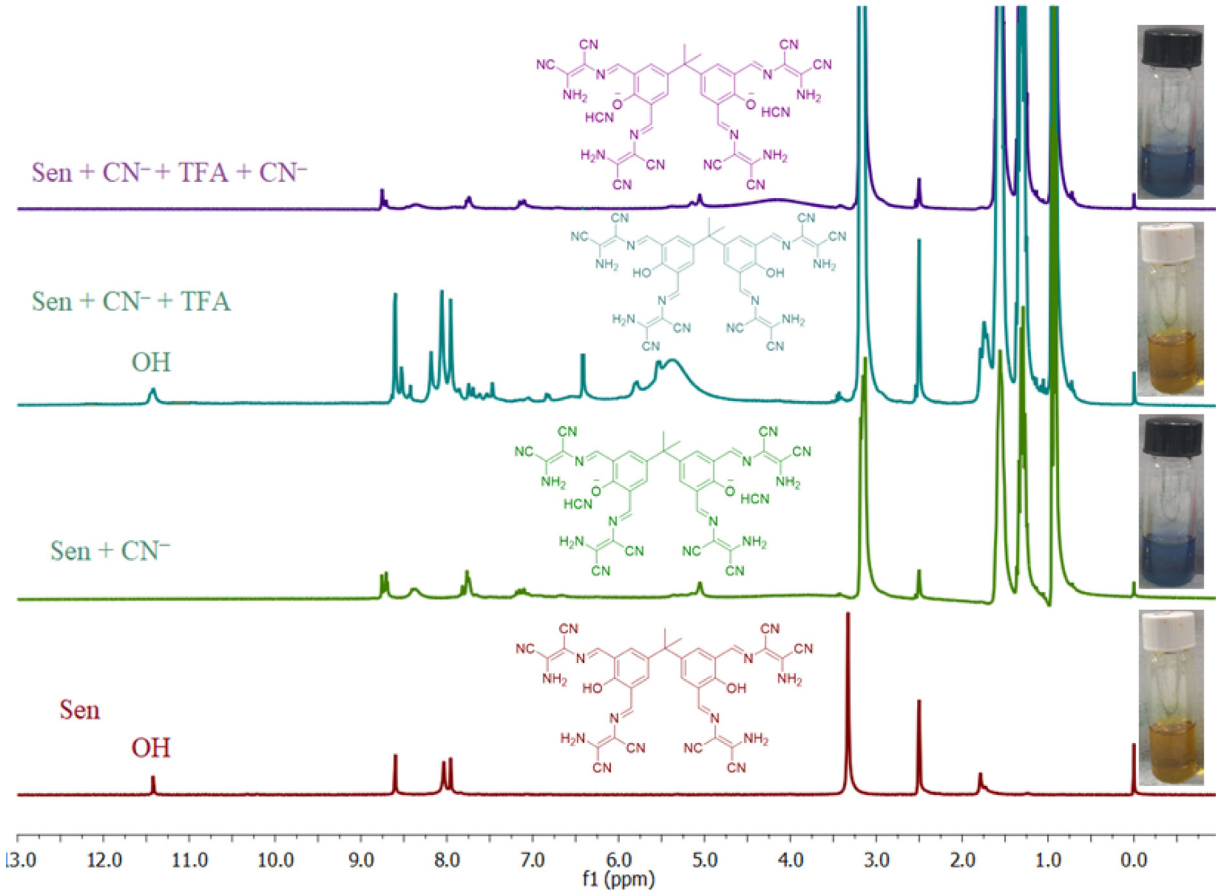

Fig. 6. ^{1}H NMR spectra analysis of deprotonation mechanism.

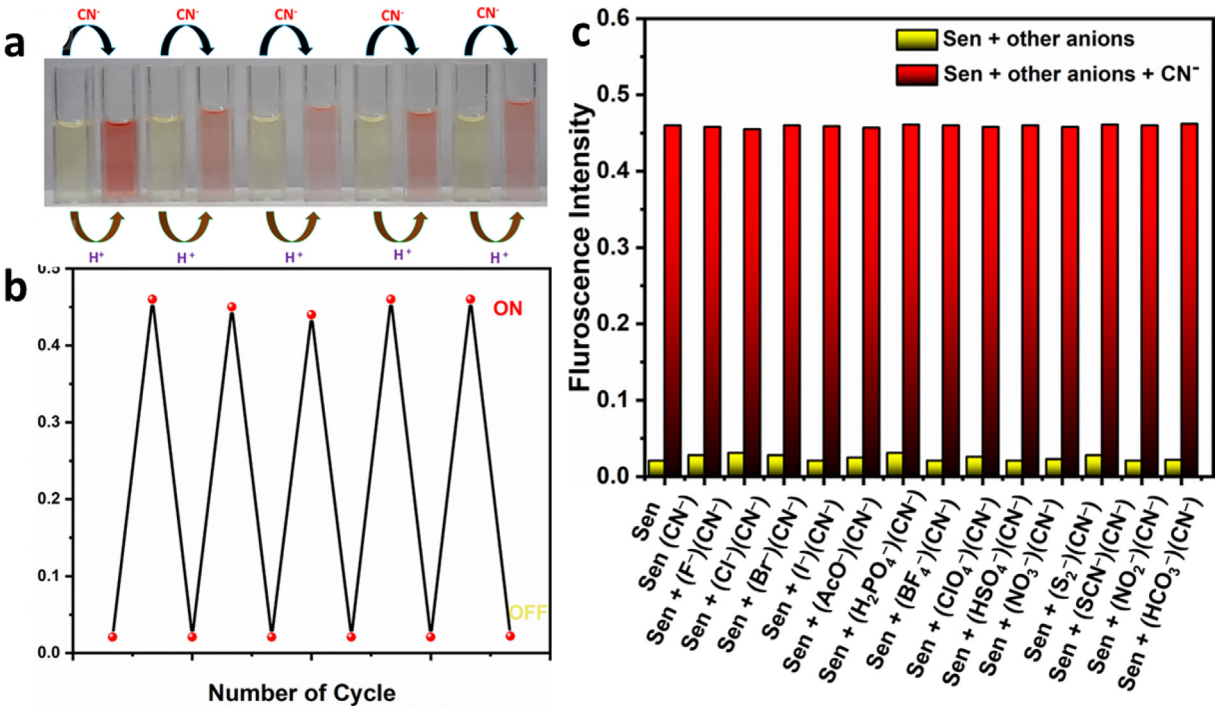

Fig. 7. (a) Alternative color change detection of **Sen** (30 μM) upon addition of the CN^- ion (60 μM) followed by TFA (30 equiv.). (b) Relative emission spectra of Sen with the sequential addition of CN^- ion and TFA. (c) Bar graph of emission spectra of interference.

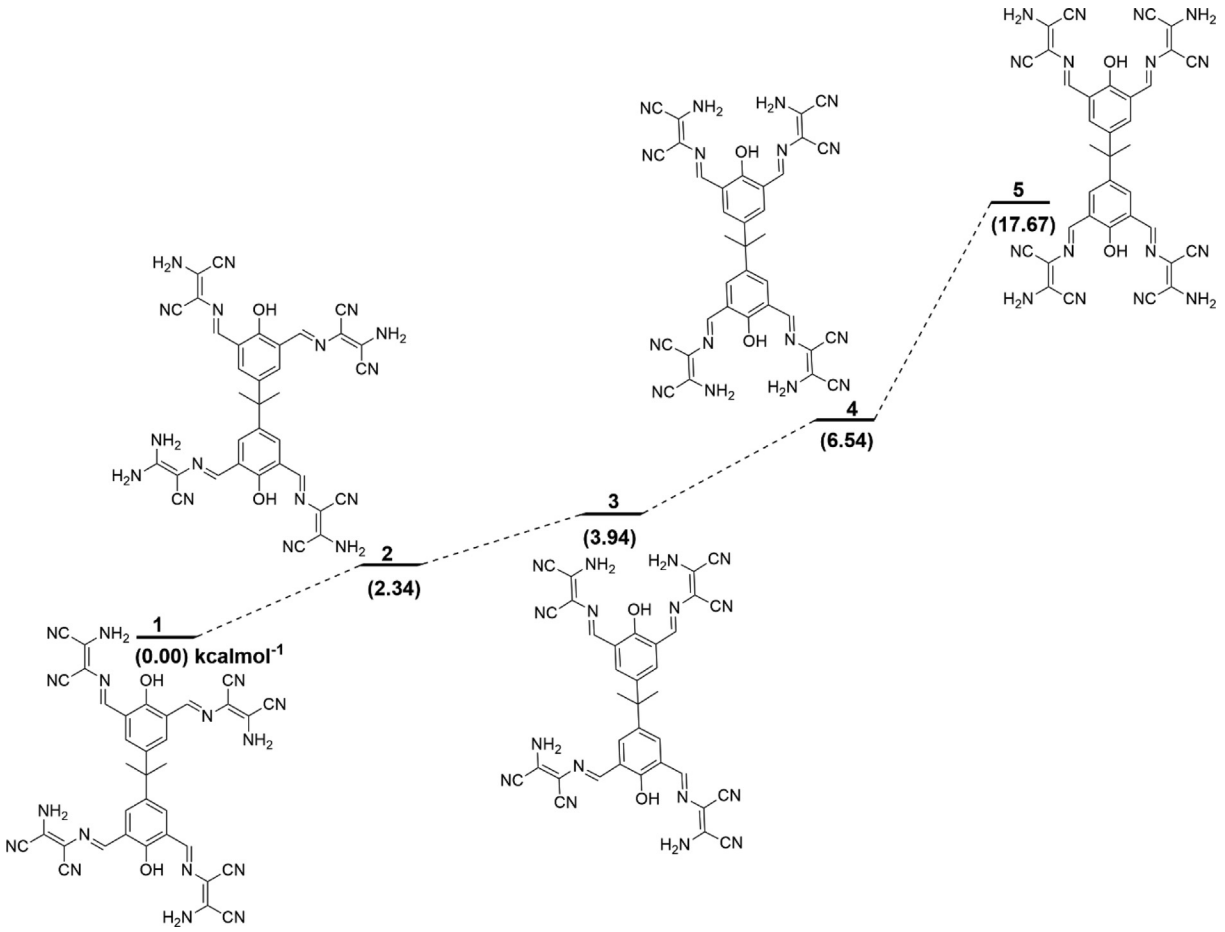

Fig. 8. Potential energy profile of conformational isomers (energies are in kcal mol^{-1}).

4. Conclusion

In conclusion, this bilateral sensor (**Sen**) is an interesting structural example of a probe with two identical sites that can operate independently. It can be synthesized on a multi-gram scale with 90% yield. It exhibits high selectivity towards the CN^- ion in DMSO/water (V/V 50%); it displays a reusable nature. The limit of detection was found to be 0.38 μM, evident through both the spectroscopic and absorption modes. The aspects of CN^- and bisphenol taken together is suggestive of future studies of biological systems in the context of research fields such as neuroscience and environmental contamination. As a consequence, the development of this optical sensor provides a facile, fast, and economic method for the optical detection and quantification of CN−.

CRediT authorship contribution statement

Zakir Ullah: Data curation, Formal analysis, Conceptualization, Methodology, Writing - original draft. **Prasad M. Sonawane:** Data curation, Formal analysis, Methodology, Resources, Software. **Thien S. Nguyen:** Data curation, Investigation, Methodology, Validation, Writing - review & editing. **Mousumi Garai:** Data curation, Investigation, Methodology, Validation, Writing - review & editing. **David G. Churchill:** Conceptualization, Investigation, Methodology, Project administration, Resources, Software, Supervision, Writing - original draft, Writing - review & editing. **Cafer T. Yavuz:** Conceptualization, Funding acquisition, Investigation, Methodology, Project administration, Resources, Software, Supervision, Writing - original draft, Writing - review & editing.

Declaration of Competing Interest

The authors declare that they have no known competing financial interests or personal relationships that could have appeared to influence the work reported in this paper.

Acknowledgment

This work was supported by the National Research Foundation of Korea (NRF) grants funded by the Korean government (MSIP) (No. NRF-2017M3A7B4042140 and NRF-2017M3A7B4042235) and the start-up funds provided by the King Abdullah University of Science and Technology (KAUST). D.G.C appreciates financial support and resources from KAIST and the International Joint Usage Project with ICR, Kyoto University (2019-115 and 2020-124) for the operation of the Molecular Logic Gate Laboratory to make this work possible. P.M.S. acknowledges the KGSP of Korea.

Appendix A. Supplementary material

Supplementary data to this article can be found online at https://doi.org/10.1016/j.saa.2021.119881.

References

[1] P.A. Gale, T. Gunnlaugsson, Preface: supramolecular chemistry of anionic species themed issue, Chem. Soc. Rev. 39 (10) (2010) 3595–3596.
[2] S.N. Kodlady, B. Narayana, B. Sarojini, S.N. Karanth, B. Gauthama, A highly selective chemosensor derived from benzamide hydrazones for the detection

of cyanide ion in organic and organic-aqueous media: design, synthesis, sensing and computational studies, Supramol. Chem. 32 (8) (2020) 433–444.
[3] P.A. Gale, C. Caltagirone, Anion sensing by small molecules and molecular ensembles, Chem. Soc. Rev. 44 (13) (2015) 4212–4227.
[4] D. Tamilarasan, R. Suhasini, V. Thiagarajan, R. Balamurugan, Reversible Addition of Cyanide to Triphenylamine Attached Difluoroboron β-Diketonate Facilitated Selective Colorimetric and Fluorimetric Detection of Cyanide Ion, Eur. J. Org. Chem. 2020 (8) (2020) 993–1000.
[5] S. Erdemir, S. Malkondu, On-site and low-cost detection of cyanide by simple colorimetric and fluorogenic sensors: smartphone and test strip applications, Talanta 207 (2020) 120278.
[6] J.-F. Chen, Q. Lin, Y.-M. Zhang, H. Yao, T.-B. Wei, Pillararene-based fluorescent chemosensors: recent advances and perspectives, Chem. Commun. 53 (100) (2017) 13296–13311.
[7] D.L. Ma, H.Z. He, K.H. Leung, D.S.H. Chan, C.H. Leung, Angewandte Chemie Int. Edition 52 (2013) 7666.
[8] Y. Singh, T. Ghosh, Highly selective colorimetric and fluorometric chemosensor for cyanide on silica gel and DMSO/H_2O (7: 3 v/v) mixed solvent and its imaging in living cells, Talanta 148 (2016) 257–263.
[9] D.L. Ma, H.Z. He, K.H. Leung, D.S.H. Chan, C.H. Leung, Bioactive luminescent transition-metal complexes for biomedical applications, Angewandte Chemie Int. Edition 52 (30) (2013) 7666–7682.
[10] A. Kumar, H.-S. Kim, A pyrenesulfonyl-imidazolium derivative as a selective cyanide ion sensor in aqueous media, New J. Chem. 39 (2015) 2935.
[11] A. Ishii, H. Seno, K. Watanabe-Suzuki, O. Suzuki, T. Kumazawa, Determination of cyanide in whole blood by capillary gas chromatography with cryogenic oven trapping, Anal. Chem. 70 (1998) 4873.
[12] World Health Organization, 2011; C.-B. Bai, J. Zhang, R. Qiao, Q.-Y. Zhang, M.-Y. Mei, M.-Y. Chen, B. Wei, C. Wang, C.-Q. Qu., Reversible and selective turn-on fluorescent and naked-eye colorimetric sensor to detect cyanide in tap water, food samples, and living systems. Industrial & Engineering Chemistry Research 2020, 59, 8125-8135.
[13] C.-B. Bai, J. Zhang, R. Qiao, Q.-Y. Zhang, M.-Y. Mei, M.-Y. Chen, B. Wei, C. Wang, C.-Q. Qu, Reversible and selective turn-on fluorescent and naked-eye colorimetric sensor to detect cyanide in tap water, food samples, and living systems, Ind. Eng. Chem. Res. 59 (2020) 8125.
[14] Y.M. Hijji, G. Wairia, A. Edwards, M. Iwunze, A.P. Kennedy Sr, R. J, Williams, in Smart Medical and Biomedical Sensor Technology II Vol. 5588 (2004) 214.
[15] Y. Hijji, G. Wairia, Smart Medical and Biomedical Sensor Technology III Vol. 6007 (2005) 60070B.
[16] S. Devaraj, D. Saravanakumar, M. Kandaswamy, Dual chemosensing properties of new anthraquinone-based receptors toward fluoride ions, Tetrahedron Lett. 48 (2007) 3077.
[17] D.H. Lee, K.H. Lee, J.-I. Hong, An azophenol-based chromogenic anion sensor, Org. Lett. 3 (2001) 5.
[18] D.H. Lee, H.Y. Lee, K.H. Lee, J.-I. Hong, Selective anion sensing based on a dual-chromophore approach, Chem. Commun. (2001) 1188.
[19] X. Zhang, L. Guo, F.-Y. Wu, Y.-B. Jiang, Development of fluorescent sensing of anions under excited-state intermolecular proton transfer signaling mechanism, Org. Lett. 5 (2003) 2667.
[20] S.K. Kim, J.H. Bok, R.A. Bartsch, J.Y. Lee, J.S. Kim, A fluoride-selective PCT chemosensor based on formation of a static pyrene excimer, Org. Lett. 7 (2005) 4839.
[21] P.A. Gale, Amidopyrroles: from anion receptors to membrane transport agents, Chem. Commun. 3761 (2005).
[22] S. Camiolo, P.A. Gale, M.B. Hursthouse, M.E. Light, C.N. Warriner., 2, 5-Diamidofuran anion receptors. Tetrahedron letters 2003, 44, 1367.
[23] Y. Wu, X. Peng, J. Fan, S. Gao, M. Tian, J. Zhao, S. Sun, Fluorescence sensing of anions based on inhibition of excited-state intramolecular proton transfer, J. Organic Chem. 72 (2007) 62.
[24] E.J. Cho, B.J. Ryu, Y.J. Lee, K.C. Nam, Visible colorimetric fluoride ion sensors, Org. Lett. 7 (2005) 2607.
[25] A.B. Descalzo, K. Rurack, H. Weisshoff, R. Martínez-Máñez, M.D. Marcos, P. Amorós, K. Hoffmann, J. Soto, Rational design of a chromo-and fluorogenic hybrid chemosensor material for the detection of long-chain carboxylates, J. Am. Chem. Soc. 127 (2005) 184.
[26] E.J. Cho, J.W. Moon, S.W. Ko, J.Y. Lee, S.K. Kim, J. Yoon, K.C. Nam, A new fluoride selective fluorescent as well as chromogenic chemosensor containing a naphthalene urea derivative, J. Am. Chem. Soc. 125 (2003) 12376.
[27] D.E. Gómez, L. Fabbrizzi, M. Licchelli, E. Monzani, Urea vs. thiourea in anion recognition, Organic Biomol. Chem. 3 (2005) 1495.
[28] D.A. Jose, D.K. Kumar, B. Ganguly, A. Das, Urea and thiourea based efficient colorimetric sensors for oxyanions, Tetrahedron Lett. 46 (2005) 5343.
[29] K. Chellappan, N.J. Singh, I.C. Hwang, J.W. Lee, K.S. Kim, A calix [4] imidazolium [2] pyridine as an anion receptor, Angewandte Chemie Int. Ed. 44 (2005) 2899.
[30] J.L. Sessler, S. Camiolo, P.A. Gale, Pyrrolic and polypyrrolic anion binding agents, Coord. Chem. Rev. 240 (2003) 17.
[31] P.A. Gale., Anion and ion-pair receptor chemistry: highlights from 2000 and 2001 Coordination chemistry reviews 2003, 240, 191.
[32] H. Tong, G. Zhou, L. Wang, X. Jing, F. Wang, J. Zhang, Novel highly selective anion chemosensors based on 2, 5-bis (2-hydroxyphenyl)-1, 3, 4-oxadiazole. Tetrahedron Lett. 2003, 44, 131.
[33] (a) T.H. Kim, C.-H. Lee, C.G. Kwak, M.S. Choi, W.H. Park, T.S. Lee, Bis (2-hydroxyphenyl)-1, 3, 4-oxadiazole derivative for anion sensing and fluorescent patterning. Molecular Crystals and Liquid Crystals 2007, 463, 255; (b) N. Ahfad, G. Mohammadnezhad, S. Meghdadi, H. Farrokhpour. A naphthylamide based fluorescent probe for detection of Al3+, Fe3+, and CN− with high sensitivity and selectivity, Spectrochim. Acta Part A: Mol. Biomol. Spectrosc. 228 (2020) 117753; (c) J. Kang, F. Huo, Y. Zhang, J. Chao, T.E. Glass, C. Yin, A novel near-infrared ratiometric fluorescent probe for cyanide and its bioimaging applications, Spectrochim. Acta Part A: Mol. Biomol. Spectrosc. 209 (2019) 95–99; (d) P. Raja Lakshmi, P. Jayasudha, Kuppanagounder P. Elango, Selective chromogenic detection of cyanide in aqueous solution –Spectral, electrochemical and theoretical studies, Spectrochim. Acta Part A: Mol. Biomol. Spectrosc. 213 (2019) 318–323.
[34] F.-Y. Wu, Z. Li, L. Guo, X. Wang, M.-H. Lin, Y.-F. Zhao, Y.-B. Jiang, A unique NH-spacer for N-benzamidothiourea based anion sensors. Substituent effect on anion sensing of the ICT dual fluorescent N-(p-dimethylaminobenzamido)-N′-arylthioureas, Organic & Biomol. Chem. 4 (2006) 624–630.
[35] G. Yang, X. Jin, K. Chen, D. Yang, Hydrogen bonding interactions induced excited state proton transfer and fluoride anion sensing mechanism for 2-(3,5-dichloro-2,6-dihydroxy-phenyl)-benzoxazole-5-carboxylicacid, J. Phys. Org. Chem. 33 (2020) e4054.
[36] J. Cho, P. Verwilst, M. Kang, J.-L. Pan, A. Sharma, C.S. Hong, J.S. Kim, S. Kim, Crown ether-appended calix [2] triazolium [2] arene as a macrocyclic receptor for the recognition of the H 2 PO 4− anion, Chem. Commun. 56 (2020) 1038.
[37] D.C. Harris, Quantitative Chemical Analysis, Macmillan, 2010.
[38] A. Al-Azmi, A.-Z.A. Elassar, B.L. Booth, The chemistry of diaminomaleonitrile and its utility in heterocyclic synthesis, Tetrahedron 59 (2003) 2749.
[39] C. Lee, W. Yang, R.G. Parr, Development of the Colle-Salvetti correlation-energy formula into a functional of the electron density. Phys. Rev. B 1988, 37 (2), 785; A.D. Becke, Density-functional exchange-energy approximation with correct asymptotic behaviour, Phys. Rev. A 1988, 38 (6), 3098.
[40] Gaussian 16, Revision A.03, M. J. Frisch, G. W. Trucks, H. B. Schlegel, G. E. Scuseria, M. A. Robb, J. R. Cheeseman, G. Scalmani, V. Barone, G. A. Petersson, H. Nakatsuji, X. Li, M. Caricato, A. V. Marenich, J. Bloino, B. G. Janesko, R. Gomperts, B. Mennucci, H. P. Hratchian, J. V. Ortiz, A. F. Izmaylov, J. L. Sonnenberg, D. Williams-Young, F. Ding, F. Lipparini, F. Egidi, J. Goings, B. Peng, A. Petrone, T. Henderson, D. Ranasinghe, V. G. Zakrzewski, J. Gao, N. Rega, G. Zheng, W. Liang, M. Hada, M. Ehara, K. Toyota, R. Fukuda, J. Hasegawa, M. Ishida, T. Nakajima, Y. Honda, O. Kitao, H. Nakai, T. Vreven, K. Throssell, J. A. Montgomery, Jr., J. E. Peralta, F. Ogliaro, M. J. Bearpark, J. J. Heyd, E. N. Brothers, K. N. Kudin, V. N. Staroverov, T. A. Keith, R. Kobayashi, J. Normand, K. Raghavachari, A. P. Rendell, J. C. Burant, S. S. Iyengar, J. Tomasi, M. Cossi, J. M. Millam, M. Klene, C. Adamo, R. Cammi, J. W. Ochterski, R. L. Martin, . Morokuma, O. Farkas, J. B. Foresman, and D. J. Fox, Gaussian, Inc., Wallingford CT, 2016.
[41] C. Bernini, L. Zani, M. Calamante, G. Reginato, A. Mordini, M. Taddei, R. Basosi, A. Sinicropi, Excited state geometries and vertical emission energies of solvated dyes for DSSC: a PCM/TD-DFT benchmark study, J. Chem. Theory Comput. 10 (9) (2014) 3925–3933.
[42] H. Khanmohammadi, A. Abdollahi, New diaminomaleonitrile-based azo-azomethine dyes; synthesis, characterization and spectral properties, Dyes Pigm. (2012).